

Leading and Trailing Anvil Clouds of West African Squall Lines

JASMINE CETRONE AND ROBERT A. HOUZE JR.

Department of Atmospheric Sciences, University of Washington, Seattle, Washington

(Manuscript received 10 June 2010, in final form 5 January 2011)

ABSTRACT

The anvil clouds of tropical squall-line systems over West Africa have been examined using cloud radar data and divided into those that appear ahead of the leading convective line and those on the trailing side of the system. The leading anvils are generally higher in altitude than the trailing anvil, likely because the hydrometeors in the leading anvil are directly connected to the convective updraft, while the trailing anvil generally extends out of the lower-topped stratiform precipitation region. When the anvils are subdivided into thick, medium, and thin portions, the thick leading anvil is seen to have systematically higher reflectivity than the thick trailing anvil, suggesting that the leading anvil contains numerous larger ice particles owing to its direct connection to the convective region. As the leading anvil ages and thins, it retains its top. The leading anvil appears to add hydrometeors at the highest altitudes, while the trailing anvil is able to moisten a deep layer of the atmosphere.

1. Introduction

Satellite data show that a large portion of upper-level-cloud ice clouds in the tropics originate as anvil clouds associated with precipitating deep convection (Luo and Rossow 2004; Kubar et al. 2007; Yuan and Hartmann 2008; Yuan et al. 2008; Yuan and Houze 2010). The largest deep convective systems (other than tropical cyclones) are mesoscale convective systems (MCSs), defined by their broad cold cloud tops and wide precipitation areas (Houze 2004). MCSs contain both active deep convective cells with heavy local precipitation and vertically towering radar echoes and more lightly raining but much broader stratiform rain areas, with horizontally stratified radar echo exhibiting a bright band at the melting level. Anvil clouds may extend outward from either the deep active precipitation cells or the wider stratiform region. This paper seeks to distinguish the properties of these two types of anvils.

We make this distinction by considering squall-line MCSs, which are organized such that their convective cells occur in a leading line of new active cells followed by a region of stratiform precipitation formed by both decaying older convective cells and by broad mesoscale

layer ascent (Zipser 1969, 1977; Houze 1977; Houze et al. 1989). We take advantage of a set of data collected at Niamey, Niger, as part of the African Monsoon Multi-disciplinary Analyses (AMMA) field program of summer 2006 (see Redelsperger et al. 2006). Situated at this field site were two radars: a C-band (5-cm wavelength) ground-based radar operated by the Massachusetts Institute of Technology (MIT), see Russel et al. (2010), which tracked the precipitation features over the Niamey region, and a vertically pointing W-band (3-mm wavelength) radar (WACR), see Mead and Widener (2005), which detected the anvil clouds ahead of and behind the passing squall systems. Cetrone and Houze (2009) analyzed the WACR data and found the anvils at Niamey to be consistent with CloudSat's Cloud Profiling Radar observations obtained in the same region.

West Africa is a region of frequent occurrence of tropical squall-line systems (Hamilton and Archbold 1945; Eldridge 1957; Payne and McGarry 1977; Fortune 1980; Martin and Schreiner 1981; Houze and Betts 1981; Sommeria and Testud 1984; Chong et al. 1987; Roux 1988; Chong and Hauser 1989; Rowell and Milford 1993; Hodges and Thorncroft 1997; Fink and Reiner 2003; Schumacher and Houze 2006; Futyán and Del Genio 2007). It is easy to determine from scanning precipitation radar data when such a system passes over a site. We therefore used the MIT radar data to subdivide the WACR data into leading and trailing anvils datasets to characterize the two types of anvil cloud.

Corresponding author address: Robert Houze, Department of Atmospheric Sciences, University of Washington, Box 351640, Seattle, WA 98195-1640.
E-mail: houze@u.washington.edu

Differences in ice cloud altitudes can affect the amount of radiative heating in the anvil clouds (e.g., Ackerman et al. 1988) of MCSs, which helps determine the total heating (latent plus radiation) of these systems. Water vapor injected into the upper troposphere by anvils also affects the transfer of infrared radiation through the uncloudy atmosphere. Higher mid-to-upper-level humidity is associated with more frequent convection (Soden and Fu 1995) and can be caught in the large-scale flow and transported to the subtropics, where the moisture can radiatively cool and subside to lower altitudes (Salathé and Hartmann 1997). Midlevel moisture is a driver of tropical cyclogenesis (DeMaria et al. 2001), and this factor is of significant importance around West Africa as approximately half of the Atlantic tropical cyclones occur when African easterly waves propagate off of the continent (Burpee 1972; Reed et al. 1977, 1988; Thorncroft and Hodges 2001). The addition of moisture by the West African squall lines (and other tropical MCSs) at a variety of levels may thus be an important precursor to a wide range of atmospheric phenomena downstream. The goal of this study, in which we separate the characteristics of the leading convective anvil and trailing stratiform anvils of squall line systems, is to determine how the convective and stratiform portions of MCSs form anvil clouds and how these regions contribute to the distribution of ice and water vapor as a function of height in the tropical troposphere.

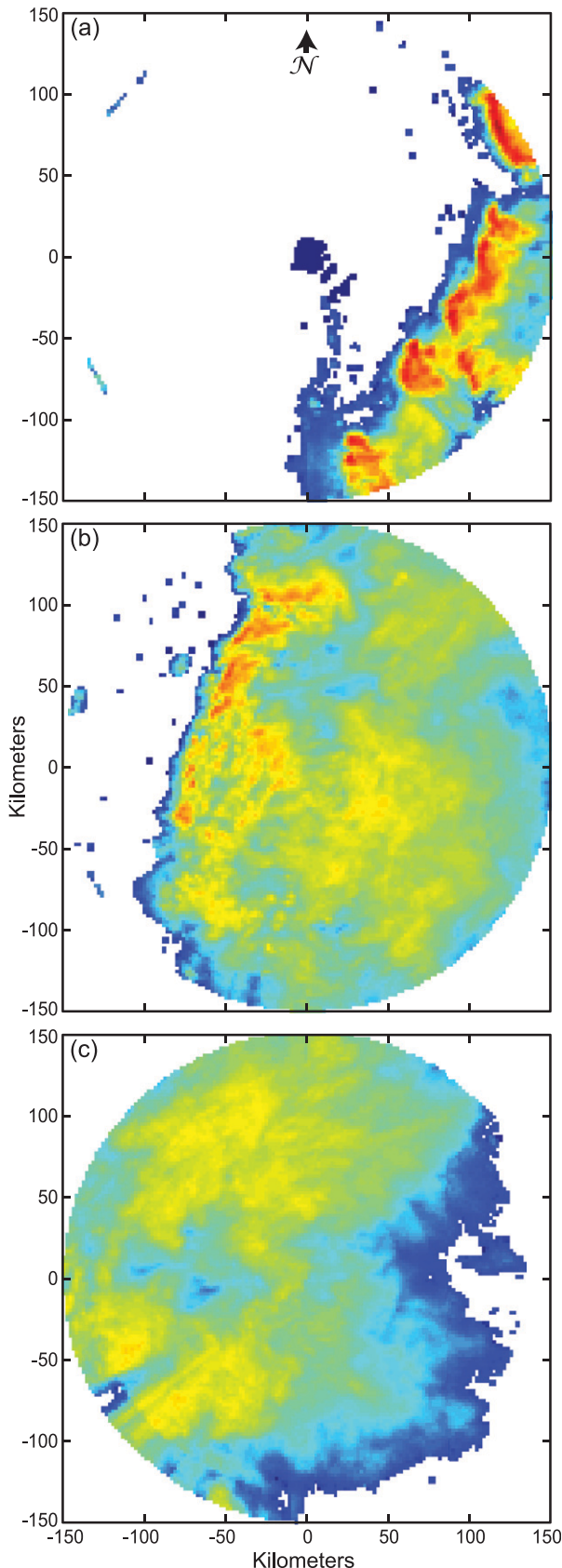
2. Data and methods of analysis

Data collected by the MIT C-band radar during 1 July–27 September 2006 were used to identify MCSs passing over Niamey. Infrared geostationary satellite data (*Meteosat-8*) were used to track the systems back to their origins and to their final destinations. An example of a squall-line MCS on the MIT radar is shown in Fig. 1. A line of intense convection is followed by a region of weaker, more uniform stratiform precipitation. Following Houze (1993), a system is identified as an MCS if its contiguous precipitation region exceeds 100 km in any direction. If part of the system was outside the radar's range, the infrared satellite data was used to determine if the system indeed met the 100-km criterion. Precipitation regions were associated with cold cloud tops (those with brightness temperatures < 208 K), consistent with the brightness temperature thresholds used previously to identify active precipitating areas (Maddox 1980; Mapes and Houze 1992; Chen et al. 1996). Squall-line MCSs are distinguished by their leading-line/trailing-stratiform precipitation pattern and rapid propagation, generally 10 – 20 m s^{-1} (Hamilton and Archbold 1945; Eldridge 1957; Zipser 1969, 1977; Aspliden et al. 1976; Houze 1977; Payne

and McGarry 1977; Fortune 1980; Hodges and Thorncroft 1997; Laing et al. 2008; Rickenbach et al. 2009; Nieto-Ferreira et al. 2009; DeLonge et al. 2010). The 15 MCSs observed in this study by the MIT radar all had leading-line/trailing-stratiform structure and convective line speeds > 13 m s^{-1} .

The WACR has a sensitivity of ~ -40 dBZ at 2 km and a range resolution of ~ 45 m. It is severely attenuated in rain but sees the anvil clouds with no significant loss of signal (Widener and Mead 2004). Because our purpose is to analyze only the anvil clouds of MCSs, we filter the WACR data to include only the nonprecipitating portions of the system. A cloud was considered precipitating if its radar reflectivity exceeded -10 dBZ anywhere below 4.5 km (just below the melting level). Although it is possible that low environmental midtropospheric humidity could affect the number or size (or both) of precipitating particles and thus incorrectly categorize some of the precipitating anvil as nonprecipitating, the choice of -10 dBZ as a threshold for precipitating anvil is consistent with other ground-based millimeter-wavelength cloud radar studies (Stephens and Wood 2007; Cetrone and Houze 2009). After the precipitating portions were removed, the WACR anvil data were divided into *leading* anvils, connected to the forward side of the convection, and *trailing* anvils, located behind the stratiform region (Fig. 2) according to the tracking of echoes on the MIT radar. Cetrone and Houze found that the variability of anvil cloud structures in three distinct monsoon regions depended on the thickness of the anvils. We therefore subdivide the forward and trailing anvil clouds according to their thickness, thin anvil thickness: 0 – 2 , medium: 2 – 6 , and thick: >6 km.

The frequency distribution of radar reflectivity varies with height, and the analysis of this variation of reflectivity provides insight into the structure and microphysical processes in anvil clouds. We therefore represent the statistics of radar reflectivity in joint probability distributions showing contours of the frequency of occurrence of a given reflectivity at a given height. A contoured frequency by altitude diagram (CFAD) (Yuter and Houze 1995) is computed for each of the subcategories of MCS anvil. To facilitate comparison between different anvil categories and subcategories, each CFAD is normalized by dividing the number in each height–reflectivity bin by the total number of anvil pixels obtained by the radar. While this dataset contains the most comprehensive sample of MCS squall-line anvils, the sample size is nonetheless small by statistical standards. To test the robustness of the results based on the sample of 15 cases, we split the sample randomly into groups of 7 and 8 cases (in this way, the entire CFAD was tested) and found that these subsamples showed results consistent with the total sample of 15. Because all of the CFADs from this significance testing



were similar, the following discussion shows only the results for the full sample.

3. Anvil cloud structures

a. Overall anvil structure

Figure 3 shows the CFAD for all leading (Fig. 3a) and trailing anvils (Fig. 3b) for the West African MCSs. At first glance the CFADs for both appear similar. Both have a dominant mode of low reflectivity values at high altitudes and higher reflectivities at lower altitudes, consistent with smaller ice crystals at high altitudes and larger, aggregate particles at lower heights. These basic characteristics of anvil-cloud CFADs have been previously documented (Cetrone and Houze 2009).

One obvious difference between the leading and trailing anvil structures is their height. Trailing anvils have systematically lower tops, consistent with the notion that leading anvils are more closely connected with the intense convective updrafts. The hydrometeors in the leading anvil would be newly created, leaving less time for fallout, resulting in maximum heights. The lower anvil-top heights in the trailing anvil must be a result of the hydrometeors, after having been created by the convection, settling downward while being advected rearward across the trailing-stratiform region. The closely packed contours above ~ 13 km in Fig. 3a indicate that the leading anvil clouds all have a similar top height, while the trailing anvils (Fig. 3b) do not display this dense stacking of contours, indicating a wider range of cloud top heights. Inspection of the data for individual cases (not shown) verifies that the greater variability in cloud top heights of trailing anvil compared to the leading anvil is seen in individual cases and is not simply an artifact of sample size (see Fig. 2).

The bases of the leading and trailing anvil clouds also differ. The leading anvils rarely reach down to 6 km, while the trailing anvils are much more likely to have a lower base. This difference is consistent with the well-known characteristic that the forward outflow layer of the convective line is in a thinner, higher layer than the deep outflow of the generally front-to-rear flow of the trailing anvil region (see Fig. 1 of Houze et al. 1989).

While the reflectivity values in the leading anvil can be as high in the trailing anvil, the CFAD shows that leading anvils tend to have lower reflectivity values at higher altitudes (frequency maximum between -30 and -20 dBZ

←

FIG. 1. Radar reflectivity of the MIT C-band scanning radar located in Niamey, Niger, from the 19 Jul 2006 mesoscale convective system at (a) 0351, (b) 0621, and (c) 0811 UTC.

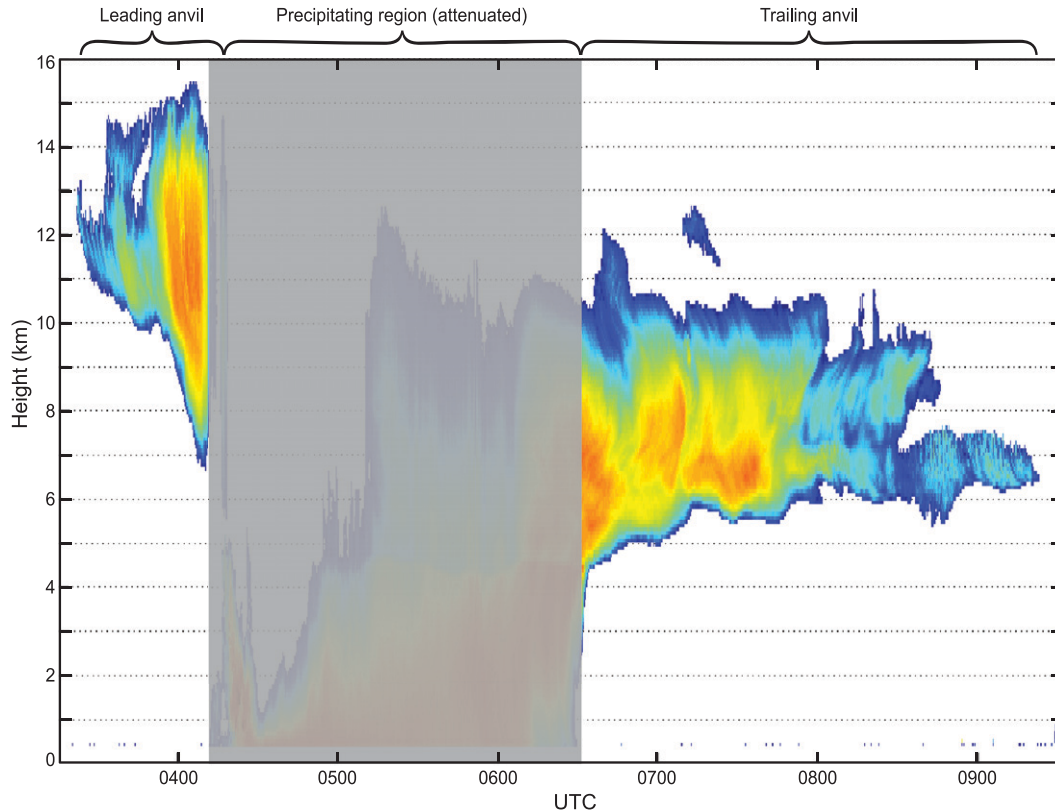


FIG. 2. Radar reflectivity of the WACR vertically pointing cloud radar located in Niamey, Niger, from the 19 Jul 2006 mesoscale convective system. Reflectivity associated with the leading anvil, trailing anvil, and precipitating regions are denoted.

at 11–14 km). Figure 3 indicates that trailing anvils are prone to higher reflectivity at lower levels (-15 to -5 dBZ at 7–10 km). Although reflectivity is weighted by particle number, its strong dependence on particle size (sixth power for Rayleigh scattering) suggests that the difference in reflectivity statistics between leading and trailing anvils is likely related to characteristic particle size, with the leading anvil containing copious amounts of small ice crystals. The hydrometeors from the trailing anvil, having had more time to settle and aggregate into larger ice crystals, have high reflectivity owing to the presence of these large snowflakes. Bouniol et al. (2010) analyzed 2D images of cloud particles from anvil clouds behind the convective line of MCSs in West Africa and found that the particles contained a high “roughness” exponent (a geometrical measurement of complexity of the image), consistent with irregular-shaped aggregates.

Trailing anvils exhibit a larger spread in frequency at all levels compared to the leading anvil. The leading anvil CFAD has one mode (low reflectivities aloft gradually shifting to higher reflectivities at lower altitudes) with a small amount of variation. The trailing anvil CFAD has a similar mode but with greater spread, especially at

lower levels. The WACR detects a significant amount of low reflectivity below 10 km in the trailing anvil, which it does not see in the leading anvil. This difference suggests that there are multiple modes in the trailing anvil system, which cannot be gleaned by simply looking at the gross anvil statistics.

Figure 4 shows a histogram of anvil thickness for both leading and trailing anvils. For both anvil types, thin anvils are most numerous. Figure 3 is thus apparently a composite of thin anvils located at various altitudes. It is therefore important to subdivide the leading and trailing anvil clouds into their varying thickness to understand the more subtle differences between these two cloud structures.

b. Thin anvils

Thin anvils (thickness < 2 km), which are located farthest from the precipitating center of the squall-line system, have grossly different CFADs depending on whether the thin anvil is on the forward or trailing side of the system (Figs. 5a,b). Since the thin anvil is at the outer edge of the system, the CFADs in Figs. 5a,b indicate that, while the leading anvil primarily injects hydrometeors into the higher-altitude environment, the trailing anvil is capable

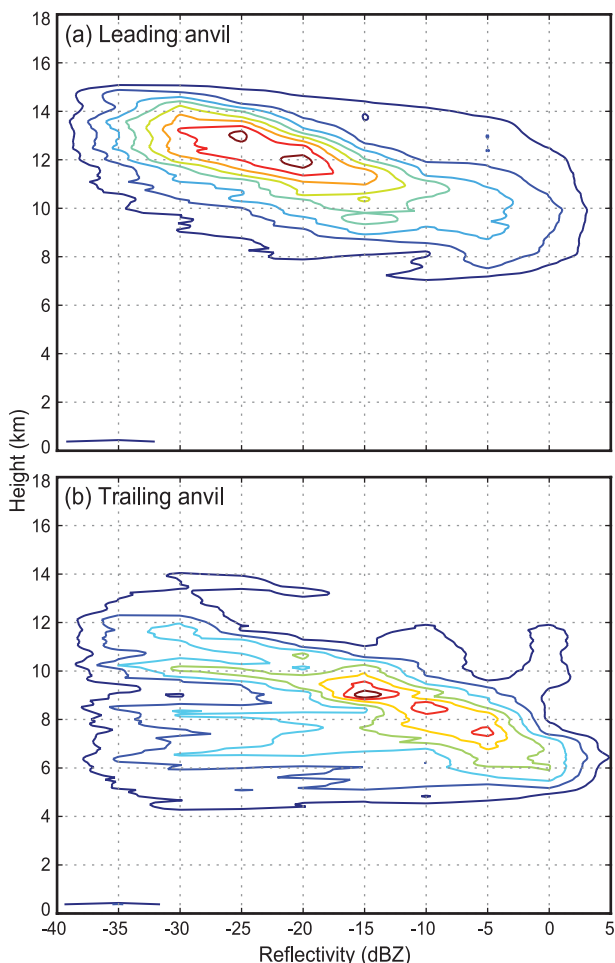


FIG. 3. CFAD showing the frequency distribution of WACR reflectivity as a function of height of an MCS (a) leading anvil and (b) trailing anvil. The contours show bin counts divided by total counts; contour interval is 0.0005 and values range from 0.0005 to 0.001. Bin dimensions are 5 dBZ by ~ 85 m.

of supplying moisture to a greater proportion of the mid- and upper troposphere.

Despite the great difference between the CFADs of leading and trailing thin anvils, one similarity is evident: the thin leading anvils have a central mode of low reflectivities (small ice) at high altitudes, centering at approximately -30 dBZ at 12 km. This mode also appears, though with a lower frequency, in the trailing thin anvils. Using *CloudSat* data, Cetrone and Houze (2009) found this upper-level mode throughout a broad spectrum of thin anvils in the tropics, though in that case the mode had a slightly higher dBZ value, likely owing to the reduced sensitivity of the spaceborne radar. The trailing thin anvil CFAD (Fig. 5b), however, indicates additional modes. A second, weaker mode appears at approximately 10 km. A third, more spread mode, with a greater frequency of higher reflectivities, is also present below 8 km. While

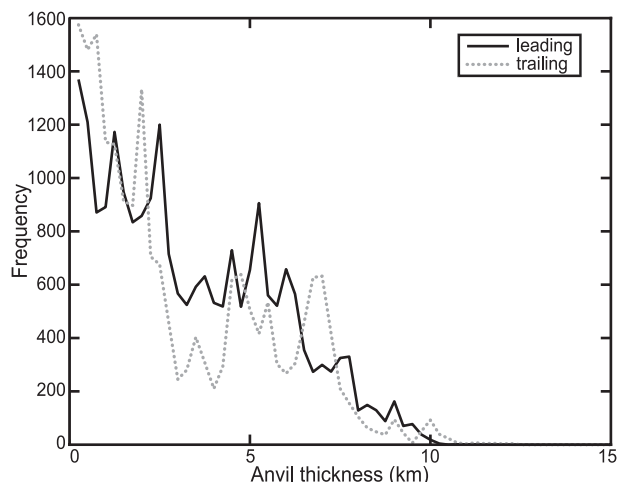


FIG. 4. Frequency distribution of MCS anvil thickness as observed by WACR for leading and trailing anvil clouds.

one could argue that these multiple modes are a meaningless sampling fluctuation owing to the small number of cases, inspection of the raw data indicated that the backs of the trailing anvil clouds tend to be ragged as the cloud dissipates unevenly at different altitudes, resulting sometimes in thin layers of residual cloud at two or even three different levels in the same system (e.g., see Fig. 2). The presence of these modes in the statistics suggests that the trailing anvils dissipate in a repeatable manner, and the thin anvils that remain at the back of the ragged edge occur at preferential altitudes. Analyzing the thin trailing anvils on a case-by-case basis shows that the lowest two modes extend for greater distances, while the highest mode generally dissipates much closer to the precipitation region. When two or more of these modes are present at the same time, it is possible that the more robust thin anvil mode at the lowest altitudes could be attenuating the signal from the higher modes, and perhaps the thin anvil at the higher altitudes is more predominant than the statistics in Fig. 5b indicate.

c. Medium anvils

Anvils of medium thickness (between 2 and 6 km) are essentially a transition between the thin and thick anvil clouds, and their associated CFADs are shown in Figs. 5c,d. For both leading and trailing anvils, the frequency distribution of anvils of medium thickness is similar to the overall CFADs for each region (Fig. 3) with a reduction in frequency of low reflectivities at high altitudes (which is an effect of the thin anvil clouds).

d. Thick anvils

Thick anvils (>6 km) over West Africa have been previously found to have a broad, flat histogram of reflectivity,

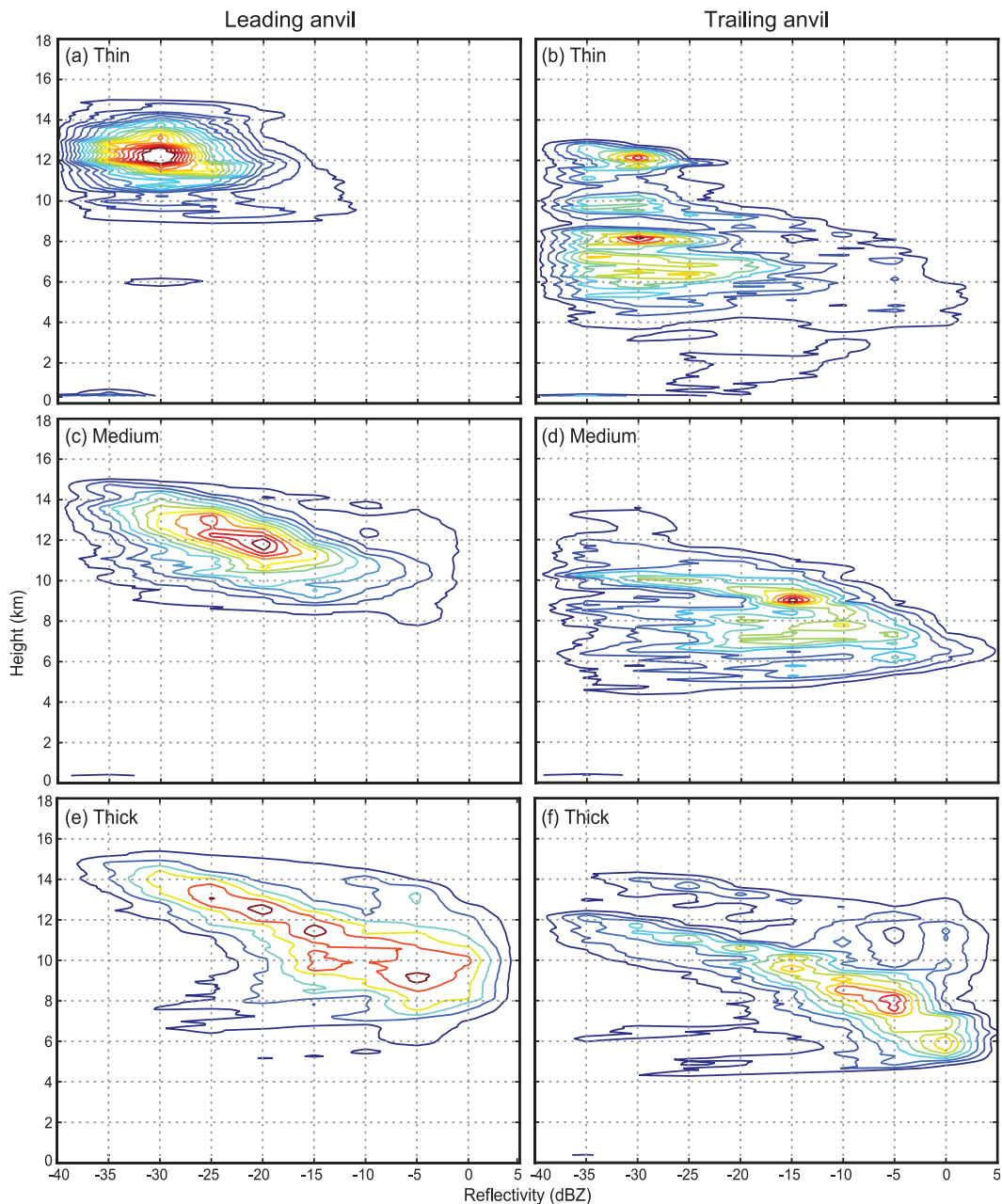


FIG. 5. As in Fig. 3, but for (a) thin (≤ 2 km) leading anvil, (b) thin trailing anvil, (c) medium (> 2 km and ≤ 6 km) leading anvil, (d) medium trailing anvil, (e) thick (> 6 km) leading anvil, and (f) thick trailing anvil.

and a maximum of reflectivity in the lower portions of the anvils (Cetrone and Houze 2009), a feature that was attributed to large ice from the intense convection being detrained into the anvils. This feature is confirmed in Figs. 5e,f. The leading thick anvil clouds are qualitatively similar to the trailing anvils but are systematically 2–4 km higher than those of the trailing anvil clouds. Thick clouds are the youngest of all anvil clouds, closest to the precipitating centers of the parent systems (e.g.,

see Fig. 2), consistent with Rickenbach et al. (2008) who observed that the tops of anvil clouds generated by convective cells decreased in altitude as the anvil aged. The leading thick anvils are tied directly to the deep convective cells of the leading convective line. This connection evidently puts them at a higher altitude compared to the trailing thick anvil extending from the trailing-stratiform region. The qualitative similarity, however, suggests that the internal dynamics and microphysics of

the anvils are similar regardless of their convective or stratiform origin.

Despite qualitative similarity, the leading and trailing thick anvils exhibit notable quantitative differences. The leading thick anvil clouds (Fig. 5e) have a broader distribution in reflectivity for a given height. Because of their direct connection with the active convection, it is reasonable that the distribution of hydrometeors would be heterogeneous—while ubiquitous small ice is injected into the leading anvils, it is likely that rimed particles are also present. That tropical Africa has an extremely high frequency of lightning and scattering of 85-GHz microwave signal (Nesbitt et al. 2000; Christian et al. 2003; Houze 2004; Cecil et al. 2005) is a clear indication that the MCSs in this region contain graupel. While it is unlikely that graupel formed in the convective updrafts would remain suspended in most trailing anvil clouds [it would be among the first particles to precipitate out in the stratiform region: in fact, Bouniol et al. (2010) found in studying in situ aircraft data in West African MCS anvils that rimed particles were fewer in number as you moved rearward in the rear anvil], graupel would likely be found in the forward anvil because of its close proximity to the updrafts. Close inspection of Figs. 5e,f shows (when comparing the thick leading anvil to the main mode in the thick trailing anvil) that above 8 km the leading anvil has systematically higher reflectivity values by ~ 5 dBZ than the trailing anvil. Below 8 km this pattern fails as there is very little thick leading anvil below 8 km, but it appears that, where the leading anvil exists, it contains either larger or more numerous (or both) particles than the trailing anvils.

The distribution for the thick trailing anvil in Fig. 5f appears to have two modes. The predominant mode is a very narrow one with tightly packed contours starting at ~ -35 dBZ at 12 km and increasing in reflectivity downward through the cloud. The concentration of contours indicates that the thick trailing anvils have little variability and that reflectivity (and therefore particle size/density) is essentially determined by the altitude. This homogeneous anvil structure with the mode descending to lower levels in the WACR cloud radar data is consistent with precipitation data obtained in the stratiform portion of the precipitating portions of MCSs (Yuter and Houze 1995; Houze et al. 2007). Yuter and Houze associated this type of CFAD structure with the classical stratiform precipitation process in which ice particles are drifting down and systematically growing by vapor deposition and undergoing aggregation to form larger-sized particles as they approach the lower part of the ice cloud.

The presence of a weaker, but still existent, second mode in the thick trailing anvils is also apparent in Fig. 5f. This is, indeed, an artifact of the small sample size, as it is related to a single squall line. It should not, however,

be ignored. The structure of the second mode is higher in altitude at all levels and actually looks somewhat similar in structure to the leading anvil CFAD in Fig. 5e. The system that produced this trailing anvil mode was a newly developed leading convective line formed by discrete propagation (Houze 2004) as an older system was dissipating. The convective line was barely an hour old when the WACR detected the anvil. Because of its young age and formation out ahead of the preexisting system, the line was not yet connected to the trailing stratiform region. The trailing anvil in this case was thus directly connected to the active convective updraft zone and was therefore similar to that of the leading anvil. This example suggests that it may not be necessarily whether the anvil is ahead of or trailing the active convective line, but rather its connection to either the convective updrafts or the stratiform precipitation that determines the anvil's structure.

4. Discussion and conclusions

The frequency distribution of cloud radar reflectivity has been computed for leading and trailing anvil clouds of 15 tropical squall-line systems over West Africa. A conceptual model summarizing the results from these data is shown in Fig. 6. The leading anvil clouds comprise hydrometeors detrained from the active convective updrafts and are systematically at higher altitude than the trailing anvil clouds.

The thick anvils (>6 km) are most closely connected to precipitation regions. On the leading side of squall systems, the thick anvils are directly tied to the convective updrafts and, besides being at a higher altitude, have a greater spread in reflectivity and generally higher reflectivity values. These characteristics are attributed to the different nature of hydrometeors in convective and stratiform regions. Intense convective updrafts of the leading line that produce the leading thick anvil likely contain heterogeneous particle types and sizes, represented by more slowly falling snow particles and more rapidly falling graupel particles in Fig. 6. In contrast, the trailing anvils are generally connected to the stratiform precipitation. Thick trailing anvil clouds are more homogeneous and lower in altitude, owing to the subsidence of smaller less-rimed particles, growing of ice by vapor deposition and aggregating to produce larger particles in the lower portions of the anvils (see Fig. 6).

As the thick anvil clouds gradually age, they become thinner as hydrometeors settle and/or sublimate. The altitudes of the medium thickness (2–6 km) and eventually thin (<2 km) clouds are related to the parent thick precipitating clouds. Thick leading anvils are higher in altitude than thick trailing anvils, and this concept holds true for thinner anvils. The leading anvil retains a similar

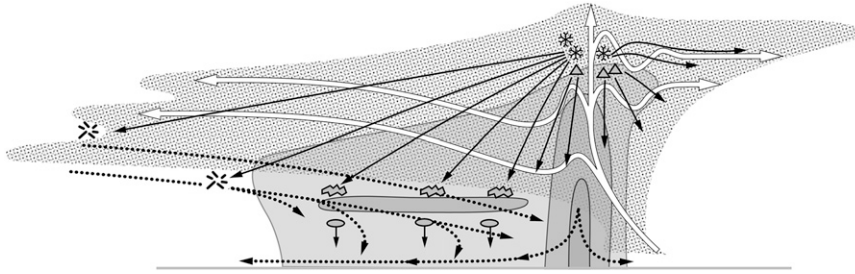


FIG. 6. Conceptual model of the kinematic, microphysical, and radar echo structure of a convective line (moving from left to right) with trailing-stratiform precipitation viewed in a vertical cross section oriented perpendicular to the convective line. The cloud structure (consistent with cloud radar data such as the WACR) is indicated by stippling. The radar echo (as it would be seen by a precipitation such as the MIT C-band) is indicated by the gray shading with intermediate and strong reflectivities indicated by medium and dark shading, respectively. The horizontal C-band radar echo maximum behind the leading line of convection is the radar bright band produced by melting of large ice particles just below the 0°C level, which is about 5 km at Niamey. The bright band distinguishes the stratiform precipitation from the convective precipitation of the leading line. The overall horizontal extent of the system would be 100–500 km. The top of the deep convective elements overshoot the tropopause. Dotted black arrows indicate mesoscale and convective-scale downdrafts; white arrows show updraft motions. Solid black arrows indicate fallout trajectories of small ice (asterisks) and graupel particles (triangles), some of which are detrained into the anvil cloud and eventually sublimate just below the trailing cloud base, and some that aggregate into snowflakes (irregularly shaped particles above the radar bright band) and eventually melt and fallout as raindrops (ovals below the bright band). Adapted from Houze et al. (1989).

top height all the way out to its forward extremity. In contrast, the top of the thick trailing anvil slopes downward toward a ragged back edge with multiple thin cloud layers protruding rearward (Fig. 6). Three modes evidently resulting from this tendency were evident in the CFAD analysis of the thin trailing anvils (Fig. 5b), indicating that the trailing anvils are capable of injecting hydrometeors and water vapor at a variety of altitudes, whereas the leading thin anvils appear to affect ice/water vapor only in the upper troposphere. The dynamics, microphysics, and life cycles of the trailing anvils connected to stratiform precipitation regions of MCSs are thus extremely important in the ability of the mesoscale cloud system to inject moisture through a deep mid-to-upper-tropospheric layer.

The results of this study may be applicable to MCSs in general—that is, not just limited to squall-line systems. A more general classification for anvil cloud (rather than leading and trailing) might be convective and stratiform anvil. When nonsquall MCSs are considered, the leading-line/trailing-stratiform paradigm, by definition, does not apply. Nonetheless, the systems comprise convective and stratiform components that exhibit many of the same properties as the convective and stratiform regions of squall-line systems. For example, Kingsmill and Houze (1999) found that the general population of MCSs over the western tropical Pacific Ocean had convective regions with up- and downdrafts similar to those seen in squall systems and that

the stratiform regions had midlevel inflow and upper-level outflow like squall systems, but with greater three-dimensionality than the quasi-two-dimensional structure of the classic tropical squall lines of the types analyzed here. Since the convective and stratiform regions of squall systems are so easy to identify, the West African systems analyzed in this study have provided an unambiguous separation of the anvil cloud data into convective and stratiform anvil types. However, we expect that the results apply broadly to the convective and stratiform elements of MCSs, whether or not the systems have squall-line organization. One application of these results is to test the output of cloud-resolving model runs of MCSs to determine whether the models accurately represent the two different types of anvils (convective and stratiform). One concern regarding generalizations, however, is that continental convective anvils may differ from oceanic convective anvils. We have cloud radar data for only one oceanic squall line. It occurred over the Bay of Bengal during the Joint Air–Sea Monsoon Interaction Experiment (JASMINE) (Webster et al. 2002). Informal analysis of this case indicates that similarities may exist between oceanic and continental squall lines. The JASMINE oceanic squall line was observed by two shipborne radars: a scanning precipitation radar (Fig. 35 of Houze 2004) and a vertically pointing cloud radar. We have plotted the CFAD of the cloud radar data (not shown) and found that the leading anvil was at a higher altitude and had

higher reflectivity values than the trailing anvil and that the trailing anvil had multiple modes in the vertical, indicating a multilayered back edge, as seen in the continental squall lines in this study. To expand the oceanic dataset beyond this one case, future joint observations by scanning precipitation radar and vertically pointing cloud radar will need to be obtained over oceanic locations.

Acknowledgments. This research was supported by the following grants: ARM-DOE Grants DE-FG02-06ER64175 and DE-SC0001164/ER-64752 and NASA Grant NNX07AQ89G. Stacy Brodzik provided invaluable data processing assistance. Beth Tully provided editing and graphics support.

REFERENCES

- Ackerman, T. P., K.-N. Liou, F. P. J. Valero, and L. Pfister, 1988: Heating rates in tropical anvils. *J. Atmos. Sci.*, **45**, 1606–1623.
- Aspliden, C. I., Y. Tourre, and J. B. Sabine, 1976: Some climatological aspects of West African disturbance lines during GATE. *Mon. Wea. Rev.*, **104**, 1029–1035.
- Bouniol, D., J. Delanoë, C. Duroure, A. Protat, V. Giraud, and C. Penide, 2010: Microphysical characterisation of West African MCS anvils. *Quart. J. Roy. Meteor. Soc.*, **136**, 323–344.
- Burpee, R. W., 1972: The origin and structure of easterly waves in the lower troposphere of North Africa. *J. Atmos. Sci.*, **29**, 77–90.
- Cecil, D. J., S. J. Goodman, D. J. Boccippio, E. J. Zipser, and S. W. Nesbitt, 2005: Three years of TRMM precipitation features. Part I: Radar, radiometric, and lightning characteristics. *Mon. Wea. Rev.*, **133**, 543–566.
- Cetrone, J., and R. A. Houze Jr., 2009: Anvil clouds of tropical mesoscale convective systems in monsoon regions. *Quart. J. Roy. Meteor. Soc.*, **135**, 305–317.
- Chen, S. S., R. A. Houze Jr., and B. E. Mapes, 1996: Multiscale variability of deep convection in relation to large-scale circulation in TOGA COARE. *J. Atmos. Sci.*, **53**, 1380–1409.
- Chong, M., and D. Hauser, 1989: A tropical squall line observed during the COPT 81 experiment in West Africa. Part II: Water budget. *Mon. Wea. Rev.*, **117**, 728–744.
- , P. Amayenc, G. Scialom, and J. Testud, 1987: A tropical squall line observed during the COPT 81 experiment in West Africa. Part I: Kinematic structure inferred from dual-Doppler radar data. *Mon. Wea. Rev.*, **115**, 670–694.
- Christian, H. J., and Coauthors, 2003: Global frequency and distribution of lightning as observed from space by the Optical Transient Detector. *J. Geophys. Res.*, **108**, 4005, doi:10.1029/2002JD002347.
- DeLonge, M. S., J. D. Fuentes, S. Chan, P. A. Kuchera, E. Joseph, A. T. Gaye, and D. Daouda, 2010: Attributes of mesoscale convective systems and the land-ocean transition in Senegal during NASA African Monsoon Multidisciplinary Analyses of 2006. *J. Geophys. Res.*, **115**, D10213, doi:10.1029/2009JD012518.
- DeMaria, M., J. A. Knaff, and B. H. Connell, 2001: A tropical cyclone genesis parameter for the Atlantic. *Wea. Forecasting*, **16**, 219–233.
- Eldridge, R. H., 1957: A synoptic study of west African disturbance lines. *Quart. J. Roy. Meteor. Soc.*, **83**, 303–314.
- Fink, A. H., and A. Reiner, 2003: Spatio-temporal variability of the relation between African Easterly Waves and West African Squall Lines in 1998 and 1999. *J. Geophys. Res.*, **108**, 4332, doi:10.1029/2002JD002816.
- Fortune, M., 1980: Properties of African squall lines inferred from time-lapse satellite imagery. *Mon. Wea. Rev.*, **108**, 153–168.
- Futyan, J., and A. Del Genio, 2007: Deep convective system evolution over Africa and the tropical Atlantic. *J. Climate*, **20**, 5041–5060.
- Hamilton, R. A., and J. W. Archbold, 1945: Meteorology of Nigeria and adjacent territory. *Quart. J. Roy. Meteor. Soc.*, **71**, 231–264.
- Hodges, K. I., and C. D. Thorncroft, 1997: Distribution and statistics of African mesoscale convective weather systems based on the ISCCP Meteosat imagery. *Mon. Wea. Rev.*, **125**, 2821–2837.
- Houze, R. A., Jr., 1977: Structure and dynamics of a tropical squall-line system. *Mon. Wea. Rev.*, **105**, 1540–1567.
- , 1993: *Cloud Dynamics*. Academic Press, 573 pp.
- , 2004: Mesoscale convective systems. *Rev. Geophys.*, **42**, RG4003, doi:10.1029/2004RG000150.
- , and A. K. Betts, 1981: Convection in GATE. *Rev. Geophys. Space Phys.*, **19**, 541–576.
- , S. A. Rutledge, M. I. Biggerstaff, and B. F. Smull, 1989: Interpretation of Doppler weather radar displays in midlatitude mesoscale convective systems. *Bull. Amer. Meteor. Soc.*, **70**, 608–619.
- , D. C. Wilton, and B. F. Smull, 2007: Monsoon convection in the Himalayan region as seen by the TRMM Precipitation Radar. *Quart. J. Roy. Meteor. Soc.*, **133**, 1389–1411.
- Kingsmill, D. E., and R. A. Houze Jr., 1999: Kinematic characteristics of air flowing into and out of precipitating convection over the west Pacific warm pool: An airborne Doppler radar survey. *Quart. J. Roy. Meteor. Soc.*, **125**, 1165–1207.
- Kubar, T. L., D. L. Hartmann, and R. Wood, 2007: Radiative and convective driving of tropical high clouds. *J. Climate*, **20**, 5510–5525.
- Laing, A. G., R. Carbone, V. Levizzani, and J. Tuttle, 2008: The propagation and diurnal cycles of deep convection in northern tropical Africa. *Quart. J. Roy. Meteor. Soc.*, **134**, 93–109.
- Luo, Z., and W. B. Rossow, 2004: Characterizing tropical cirrus life cycle, evolution, and interaction with upper-tropospheric water vapor using Lagrangian trajectory analysis of satellite observations. *J. Climate*, **17**, 4541–4563.
- Maddox, R. A., 1980: Mesoscale convective complexes. *Bull. Amer. Meteor. Soc.*, **61**, 1374–1387.
- Mapes, B. E., and R. A. Houze Jr., 1992: Satellite-observed cloud clusters in the TOGA-COARE domain. *TOGA Notes*, April 1992, 5–8.
- Martin, D. W., and A. J. Schreiner, 1981: Characteristics of West African and East Atlantic cloud clusters: A survey from GATE. *Mon. Wea. Rev.*, **109**, 1671–1688.
- Mead, J. B., and K. B. Widener, 2005: W-Band ARM cloud radar. Preprints, *32nd Conf. on Radar Meteorology*, Albuquerque, NM, Amer. Meteor. Soc., P1R.3. [Available online at ams.confex.com/ams/pdfpapers/95978.pdf.]
- Nesbitt, S. W., E. J. Zipser, and D. J. Cecil, 2000: A census of precipitation features in the tropics using TRMM: Radar, ice scattering, and ice observations. *J. Climate*, **13**, 4087–4106.
- Nieto-Ferreira, R., T. Rickenbach, N. Guy, and E. Williams, 2009: Radar observations of convective system variability in relationship to African Easterly Waves during the 2006 AMMA special observing period. *Mon. Wea. Rev.*, **137**, 4136–4150.

- Payne, S. W., and M. M. McGarry, 1977: The relationship of satellite inferred convective activity to easterly waves over West Africa and the adjacent ocean during phase III of GATE. *Mon. Wea. Rev.*, **105**, 413–420.
- Redelsperger, J. L., C. D. Thorncroft, A. Diedhiou, T. Lebel, D. J. Parker, and J. Polcher, 2006: African Monsoon Multi-disciplinary Analysis: An international research project and field campaign. *Bull. Amer. Meteor. Soc.*, **87**, 1739–1746.
- Reed, R. J., D. C. Norquist, and E. E. Recker, 1977: The structure and properties of African wave disturbances as observed during Phase III of GATE. *Mon. Wea. Rev.*, **105**, 317–333.
- , E. Klinker, and A. Hollingsworth, 1988: The structure and characteristics of African easterly wave disturbances as determined from the ECMWF operational analysis/forecast system. *Meteor. Atmos. Phys.*, **38**, 22–33.
- Rickenbach, T., P. Kucera, M. Gentry, L. Carey, A. Lare, R.-F. Lin, B. Demoz, and D. Starr, 2008: The relationship between anvil clouds and convective cells: A case study in South Florida during CRYSTAL-FACE. *Mon. Wea. Rev.*, **136**, 3917–3932.
- , R. Nieto Ferreira, N. Guy, and E. Williams, 2009: Radar-observed squall-line propagation and the diurnal cycle of convection in Niamey, Niger, during the 2006 African Monsoon and Multidisciplinary Analyses Intensive Observing Period. *J. Geophys. Res.*, **114**, D03107, doi:10.1029/2008JD010871.
- Roux, F., 1988: The West African squall line observed on 23 June 1981 during COPT 81: Kinematics and thermodynamics of the convective region. *J. Atmos. Sci.*, **45**, 406–426.
- Rowell, D. P., and J. R. Milford, 1993: On the generation of African squall lines. *J. Climate*, **6**, 1181–1193.
- Russel, B., and Coauthors, 2010: Radar/rain-gauge comparisons on squall lines in Niamey, Niger for the AMMA. *Quart. J. Roy. Meteor. Soc.*, **136**, 289–303.
- Salathé, E. P., and D. L. Hartmann, 1997: A trajectory analysis of tropical upper-tropospheric moisture and convection. *J. Climate*, **10**, 2533–2547.
- Schumacher, C., and R. A. Houze Jr., 2006: Stratiform precipitation production over sub-Saharan Africa and the tropical East Atlantic as observed by TRMM. *Quart. J. Roy. Meteor. Soc.*, **132**, 2235–2255.
- Soden, B. J., and R. Fu, 1995: A satellite analysis of deep convection, upper-tropospheric humidity, and the greenhouse effect. *J. Climate*, **8**, 2333–2351.
- Sommeria, G., and J. Testud, 1984: COPT 81: A field experiment designed for the study of dynamics and electrical activity of deep convection in continental tropical regions. *Bull. Amer. Meteor. Soc.*, **65**, 4–10.
- Stephens, G. L., and N. B. Wood, 2007: Properties of tropical convection observed by millimeter-wave radar systems. *Mon. Wea. Rev.*, **135**, 821–842.
- Thorncroft, C., and K. Hodges, 2001: African Easterly Wave variability and its relationship to Atlantic tropical cyclone activity. *J. Climate*, **14**, 1166–1179.
- Webster, P. J., and Coauthors, 2002: The JASMINE pilot study. *Bull. Amer. Meteor. Soc.*, **83**, 1603–1630.
- Widener, K. B., and J. B. Mead, 2004: W-Band ARM cloud radar—Specifications and design. *Proc. 14th ARM Science Team Meeting*, Albuquerque, NM, ARM. [Available online at http://www.arm.gov/publications/proceedings/conf14/extended_abs/widener2-kb.pdf?id=63.]
- Yuan, J., and D. L. Hartmann, 2008: Spatial and temporal dependence of clouds and their radiative impacts on the large-scale vertical velocity profile. *J. Geophys. Res.*, **113**, D19201, doi:10.1029/2007jd009722.
- , and R. A. Houze Jr., 2010: Global variability of mesoscale convective system anvil structure from A-train satellite data. *J. Climate*, **23**, 5864–5888.
- , D. L. Hartmann, and R. Wood, 2008: Dynamic effects on the tropical cloud radiative forcing and radiation budget. *J. Climate*, **21**, 2337–2351.
- Yuter, S. E., and R. A. Houze Jr., 1995: Three-dimensional kinematic and microphysical evolution of Florida cumulonimbus. Part II: Frequency distribution of vertical velocity, reflectivity, and differential reflectivity. *Mon. Wea. Rev.*, **123**, 1941–1963.
- Zipser, E. J., 1969: The role of organized unsaturated convective downdrafts in the structure and rapid decay of an equatorial disturbance. *J. Appl. Meteor.*, **8**, 799–814.
- , 1977: Mesoscale and convective-scale downdrafts as distinct components of squall-line circulation. *Mon. Wea. Rev.*, **105**, 1568–1589.